Technical Material

Effect of B_4C Absorber Material on Melt Progression and Chemical Forms of Iodine or Cesium under Severe Accident Conditions

Akihide HIDAKA [1,*,†]

[1] *Nuclear Safety Research Center, Japan Atomic Energy Agency,*
2-4 shirane, Shirakata, Tokai-mura, Naka-gun, Ibaraki 319-1195, Japan

Boron carbide (B_4C) used for BWR or EPR absorbers could cause phenomena that never occur in PWR with silver-indium-cadmium absorbers during a severe accident. B_4C would undergo a eutectic interaction with stainless steel and enhance core melt relocation. Boron oxidation could increase H_2 generation, and the change of liberated carbon to CH_4 could enhance the generation of organic iodide (CH_3I). HBO_2 generated during B_4C oxidation could be changed to cesium borate ($CsBO_2$) by combining it with cesium. This may increase cesium deposition into the reactor coolant system. There could be differences in the configuration, surface area, and stainless-steel to B_4C weight ratio between the B_4C powder absorber and pellet absorber. The present task is to clarify the effect of these differences on melt progression, B_4C oxidation, and the iodine or cesium source term. Advancement of this research field could contribute to further sophistication of prediction tools for melt progression and source terms of the Fukushima Accident, and the treatment of organic iodide formation in safety evaluation.

KEYWORDS: B_4C powder absorber, B_4C pellet absorber, eutectic reaction, organic iodide, cesium borate, melt progression, iodine source term, cesium source term

I. Introduction

Boron carbide is used as an absorber for nuclear reactors such as boiling water reactors (BWRs), European pressurized reactors (EPRs), and Russian pressurized reactors (Voda Energo Reactor/VVER). B_4C could cause phenomena during a severe accident that never occur in pressurized water reactors (PWRs) in which silver-indium-cadmium (S-I-C) absorbers are widely used, and may influence the melting of the reactor core, hydrogen generation, source terms, and other processes.

The cooling function of the reactor is lost during a severe accident, and as a result, the temperature of UO_2 fuel rods, absorber rods, and the surrounding reactor structures will increase because of insufficient removal of decay heat. During such a situation, if different types of metals or ceramics are in contact with each other, melting will start at a lower temperature

---

* Corresponding author, E-mail: hidaka.akihide@jaea.go.jp
† Currently, Nuclear Human Resource Development Center, Japan Atomic Energy Agency
DOI : 10.15669/fukushimainsights.Vol.4.341

Originally published in Transactions of the Atomic Energy Society of Japan (ISSN 1347–2879), Vol. 14, No. 1, p.51–61 (2015) in Japanese. (Japanese version accepted: October 7, 2014)

than the individual melting points due to eutectic reactions. For a B_4C control rod, the stainless steel cladding tube and B_4C (melting point 2,620 K) will liquify and flow downwards at temperatures less than the melting point of stainless steel (1,673–1,723 K). The molten substances will solidify when cooled in the lower part of the reactor core, but portions will travel further down in the reactor pressure vessel. Moreover, reaction heat, and H_2 will be generated by the oxidation of B_4C itself at around 1,500 K.

As the temperature increases further, the fuel cladding tubes and UO_2 fuel will be melted, and the molten substances will flow down around the fuel rod like candle wax (candling phenomenon) and fall down to the bottom of the reactor core or the reactor pressure vessel, as same as the case of B_4C control rods. These molten materials will finally form molten debris that contains the previously melted absorber materials and reactor core structures including the UO_2 fuel. The radioactive materials in the molten debris will react with dissolved oxygen and absorber materials in the debris, and their chemical form including melting point and boiling point will vary.

For the aforementioned reasons, a change in the absorber material influences the reactor core melting process, the quantity of H_2 generated, and the amount, kind and timing (source terms) of the radioactive materials released into the environment.

Research into progress of core melting phenomena, especially after the TMI-2 accident 1) that occurred in the USA in 1979, has focused mainly on that of PWRs using S-I-C absorbers. Through numerous international experiments, various insights into the influence of absorber materials on the progress of reactor core melting of PWRs have been obtained 2). However, only a few experiments have been done on BWRs, partly because of the small number of reactors that use B_4C absorbers. Recently, after EPRs began using the B_4C absorbers, the effect of B_4C on the chemical forms of iodine released from the fuel during a severe accident has been studied more extensively. In particular, studies have examined the association of B_4C with the generation of gaseous iodine (organic iodine, CH_3I), which is difficult to remove with containment spray or filters, and is important for the evaluation of exposure. These topics have been investigated mainly in Europe 3). Ironically, it was a BWR that caused a reactor core meltdown in the accident at TEPCO's Fukushima Dai-ichi Nuclear Power Plant 4). In the process of removing the debris from the reactor core, restoring the environment, identifying the causes and process of the reactor core meltdown, and studying the source terms in detail in the future, it is essential to understand the influence of B_4C absorbers. Based on such future needs in Japan, this study was intended to summarize the results and leftover issues of existing typical experiments to examine chemical reactions involving B_4C and the effect of B_4C absorber materials on the reactor core melting process, and the comparison between B_4C and S-I-C control rods.

II. Chemical Reactions

In a B_4C oxidation process, similar to Zr oxidation, not only are large amounts of reaction heat and H_2 generated, but also CO, CO_2, and CH_4 that may influence the chemical forms of iodine. The main chemical reactions are listed along with the Zr oxidation reaction formula, as follows: 5, 6)

Oxidation of B_4C 5)

$$B_4C + 7H_2O(g) \rightarrow 2B_2O_3 + CO(g) + 7H_2(g) \qquad \Delta H = -738\ \mathrm{kJ/mol} \qquad (1)$$

$$B_4C + 8H_2O(g) \rightarrow 2B_2O_3 + CO_2(g) + 8H_2(g) \quad \Delta H = -768\ \mathrm{kJ/mol} \tag{2}$$

$$B_4C + 6H_2O(g) \rightarrow 2B_2O_3 + CH_4(g) + 4H_2(g) \quad \Delta H = -965\ \mathrm{kJ/mol} \tag{3}$$

Reactions related to boron oxide (B_2O_3)[5]

$$B_2O_3 + H_2O(g) \rightarrow 2HBO_2(\text{metaboric acid}) \quad \Delta H = 332\ \mathrm{kJ/mol} \tag{4}$$

$$B_2O_3 + 3H_2O \rightarrow 2H_3BO_3(\text{orthoboric acid}) \quad \Delta H = -40\ \mathrm{kJ/mol} \tag{5}$$

$$B_2O_3(l) \rightarrow B_2O_3(g) \quad \Delta H = 383\ \mathrm{kJ/mol} \tag{6}$$

Reactions related to decomposition of CH_4[6]

$$CH_4(g) + H_2O(g) \rightarrow CO(g) + 3H_2(g) \quad \Delta H = 228\ \mathrm{kJ/mol} \tag{7}$$

$$CH_4(g) + 2H_2O(g) \rightarrow CO_2(g) + 4H_2(g) \quad \Delta H = 197\ \mathrm{kJ/mol} \tag{8}$$

Oxidation of Zr

$$Zr + 2H_2O(\text{steam}) \rightarrow ZrO_2 + 2H_2 \quad \Delta H = -582\ \mathrm{kJ/mol} \tag{9}$$

where, the enthalpies of the reactions in formulas (1)–(9) were calculated using the formation enthalpy at 1,500 K in the cited literature[7].

In the process of B_4C oxidation, similar to that of Zr, a partial reaction starts at around 1,473 K and rapidly progresses to more than 1,543 K[8]. Notably, the aforementioned chemical reaction formulas indicate that, relative to the oxidation of the same mass of Zr (density 6.53 g/cm^3), the reaction heat from the oxidation of B_4C (density 2.5 g/cm^3) is three to four times higher, and the quantity of hydrogen generated is six to seven times higher .

CH_3I is believed to be generated from reactions between CH_4 and HI or I_2. CH_4 is generated by the oxidation of B_4C as shown in formula (3) or generated by the reverse reactions (i.e., the reaction of H_2 and CO or CO_2) of formulas (7) and (8) in the low temperature nuclear reactor coolant system[9]. However, the detailed reaction processes involved are not well known[10]. For instance, formulas (7) and (8), which describe the decomposition of CH_4, were introduced as indicators of the small quantity of CH_4 generation in a series of experiments conducted in Europe on the individual effects of B_4C oxidation.

III. Past Experimental Studies on the Influence of B_4C Absorber Materials

This section discusses the past experiments DF-4[11, 12] and XR2-1[13], conducted by Sandia National Laboratories (SNL), USA on the control rod blades for a BWR, CORA-16[14] by Forschungszentrum Karlsruhe (FZK), Germany on the B_4C pellet control rods for an EPR, and FPT-3[9, 16-18] and BECARRE[19] conducted by the Institut de Radioprotection et de Surete Nucleaire (IRSN), France.

1. DF-4 Experiment (SNL)[11, 12]

After the TMI-2 accident, the United States Nuclear Regulatory Commission (USNRC) conducted the DF-4 experiment in 1989 as the fourth in the series of damaged fuel (DF) experiments in the Severe Fuel Damage (SFD) Program enforced during the period from 1982 to

1992 using the annular core research reactor (ACRR) of SNL. The purpose of this experiment was to acquire general information regarding the reactor core damage process in the initial stage of a severe BWR accident. The experimental core section consisted of 14 fuel rods (0.5 m long), B_4C (powder) control rods + simulated channel box (**Figure 1**), and the simulated fuel zone was heated by nuclear fission in a steam atmosphere. The measurements included the measurement of temperature by thermocouples (TC) and H_2 concentration focusing on heat generation during CuO reduction.

One of the major outcomes was the observation of melting of stainless steel at a temperature below the melting point of stainless steel due to a eutectic reaction with B_4C, and the relocation of B_4C to a lower position as a result of being captured in the molten stainless steel, and a chemical reaction involving B_4C mainly occurred at this lower position with Cs (alkali metal), Sr (alkali earth metal), and other elements. No reaction with iodine was observed before the relocation.

However, because the experimental core section was made on a small scale, further verification was required in order to apply the acquired results to real reactors.

2. XR2-1 Experiment (SNL) [13)]

The USNRC conducted an XR2-1 experiment in 1996 using an apparatus installed in an experimental vessel of the Fully Instrumented Test Site (FITS) as the third in a series of Ex-Reactor (XR) experiments. When a short-term station blackout occurs while a depressurized condition exists in the reactor coolant system of a BWR, the reactor core is expected to be in a dry core condition (i.e., the coolant remains in the bottom part of the reactor pressure vessel and only a small quantity of steam passes through the reactor core). The objective of this experiment was to investigate the reactor core melting process under such a condition. Note that, in the TMI-2 accident in which the reactor coolant system was not depressurized, it was reported that the reactor core bottom was flooded, and because of the wet core conditions, the cooling water was boiling due to the decay heat, which meant that a large quantity of steam was continuously supplied to the upper part of reactor core. As a result, a metal crust was generated at lower part of the reactor core, and the molten substances were maintained on the crust.

In the experiment, as shown in **Figure 2** and **Figure 3**, from the upper part of the testing section, which consisted of 64 fuel rods (0.5 m long) and B_4C (powder) control rods, molten substances generated by induction heating of wire Zr and stainless steel-B_4C were dropped.

The main result was that the type of large-scale metal crust found in the TMI-2 accident was not generated under the fuel rods, and the molten substances continuously dropped to the

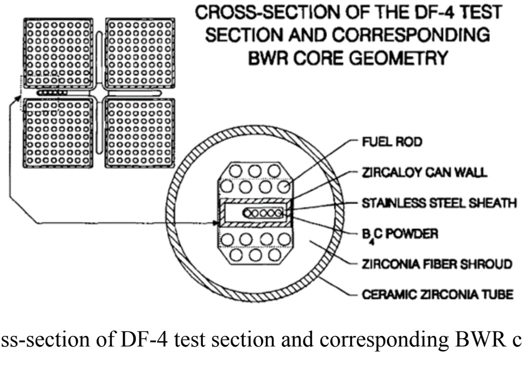

Figure 1 Cross-section of DF-4 test section and corresponding BWR core geometry [11)]

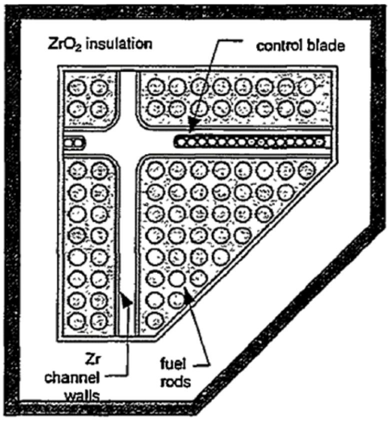

Figure 2 Cross-section of simulated reactor core of XR-2 test [13)]

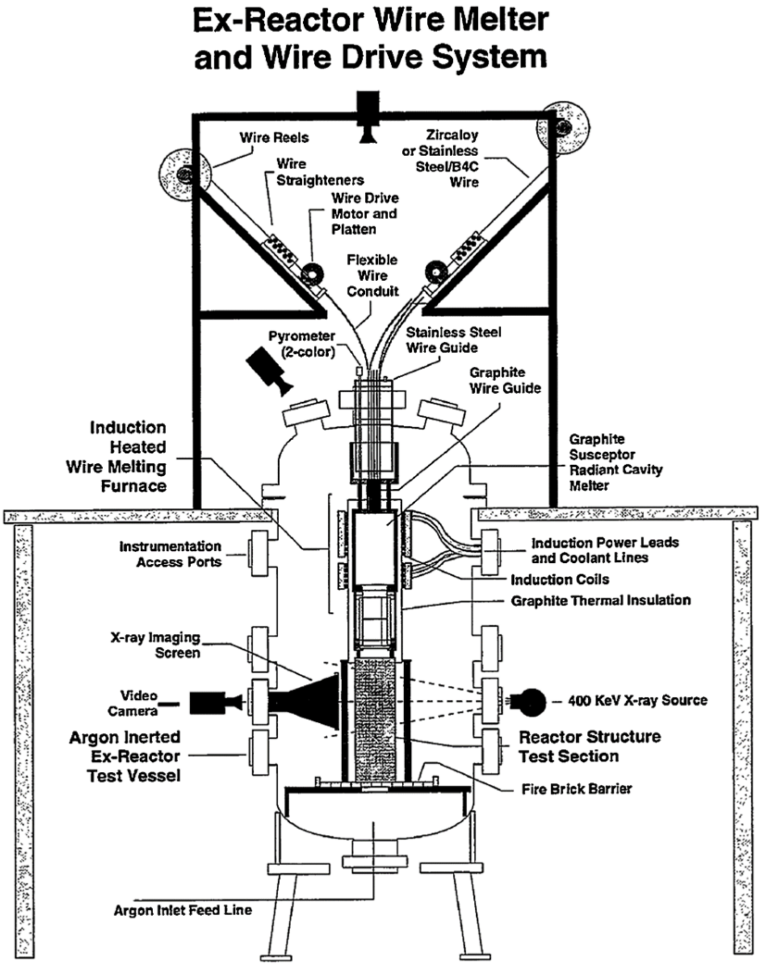

Figure 3 XR-2 experimental device installed using existing FITS (Fully Instrumented Test Site) experiment vessel [13)]

lower plenum section through the gaps between the existing structures. However, some minor blockages were caused by the molten substances. The test apparatus had a temperature gradient of 2,000 K/m in the vertical direction, and it was noted that the results might vary if the experimental conditions were changed.

Additionally, the experimental results were analyzed using the MERIS [20)] reactor core melting process analysis code that was under development at SNL, which predicted the clogged flow path in the reactor core zone with the molten materials but could not predict molten materials dropping down into the lower plenum section. This unsolved issue was reserved as a subject for future study.

3. CORA-16 Experiment (KfK) [14)]

The Nuclear Research Center Karlsruhe (KfK, presently FZK) in Germany started the PSF Program (nuclear safety research program) in January 1992 to evaluate the effectiveness of severe accident management devices that were to be installed in the EPR. In this program, the CORA experiment (Ex-Reactor experiment), to investigate the damage and melting processes of fuel assemblies, and the BETA experiment that examined the molten core concrete interaction, were performed.

The test zone of the CORA experiment consisted of simulated fuel rods implemented with an electric heater with a 1 m long heating zone, simulated fuel rods (not heated), and control rods. The main achievements of the CORA experiment were the discovery of "candling" during the heating process, the occurrence of the acceleration of oxidation of the upper fuel cladding tube in the reflooding process when the immediate prior condition was under steam starvation, and the increased release of radioactive materials due to fuel smashing during reflooding.

The influence of the BWR control rods was investigated in the CORA-16 experiment. The main findings comprised the discovery of melting of B_4C through a eutectic reaction with stainless steel at around 1,500 K, the inhibition of the reaction of B_4C by steam, and the generation of HBO_2 due to the reaction of the molten substances with the fuel cladding tube after penetrating the channel box. However, it was understood that further verification was necessary because B_4C caused melting by means of a eutectic reaction with zircalloy at over 1,920 K.

4. QUENCH-07 and QUENCH-09 Experiments (FZK) [5, 15)]

FZK Germany conducted the QUENCH experiments as a follow-up to the CORA experiments to investigate the generation behavior of H_2 during the reflooding of the fuel rods. The front view of the experimental device is shown in **Figure 4**. The simulated reactor core consists of 20 simulated fuel rods (approximately 1 m long) and a fuel rod or a control rod positioned in the center (**Figure 5**).

In the experiment, the reflooding condition was simulated by injecting water or steam from the area at the bottom of the fuel rods heated up to 2,000 K in advance. The simulated control rods used for the QUENCH-07 and QUENCH-09 experiments (conducted in 2001 and 2002, respectively) were B_4C pellets within stainless steel-clad tubes and zircalloy-4 guide tubes.

The experiments confirmed that molten boron, carbon, and Zr were generated at a lower temperature (1,520 K) than the melting point of Zr (2,030 K) through a eutectic reaction between B_4C and Zr, and the melting of the reactor core was accelerated compared to the experiments conducted with S-I-C control rods (**Figure 6**). Furthermore, it was confirmed that when the saturated steam was injected from the bottom zone of the fuel rods, H_2, CO, CO_2, and CH_4 were

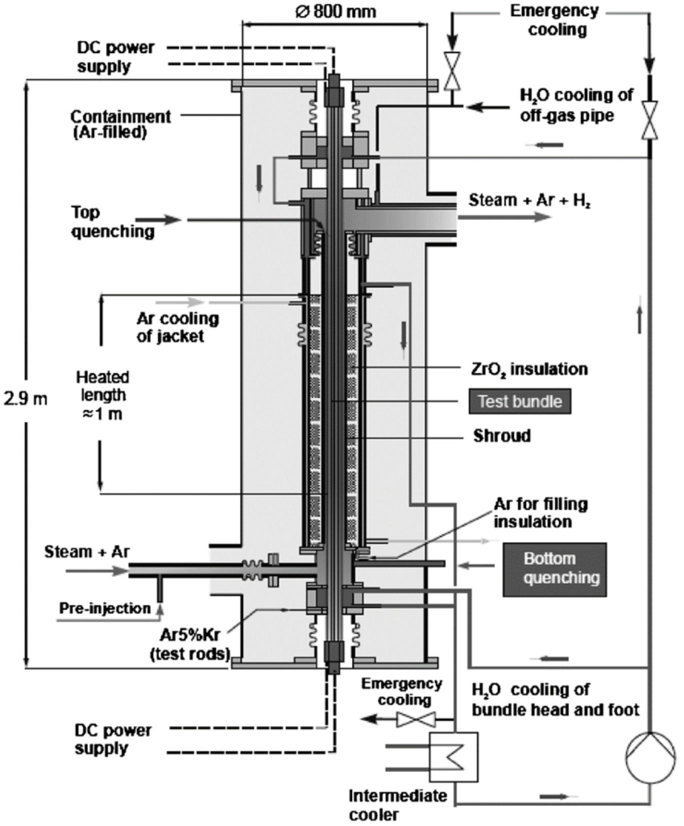

Figure 4 Front view of QUENCH experimental device [15)]

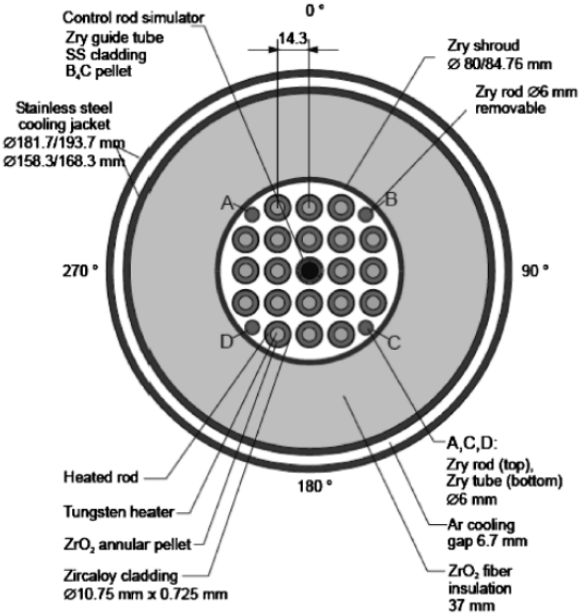

Figure 5 Cross-section of simulated reactor core for QUENCH experiment [15)]

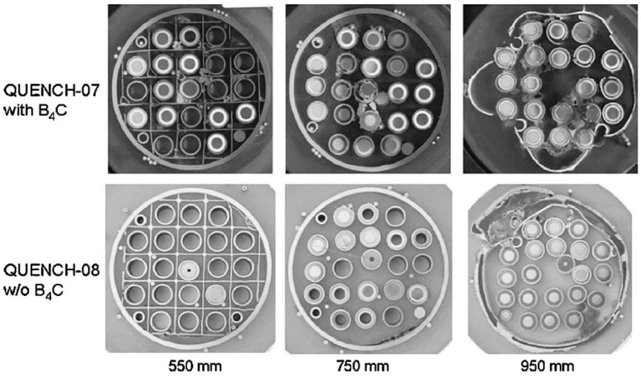

Figure 6 Comparison of cross-sections of simulated reactor core after QUENCH heating experiment between for presence and absence of B_4C 9)

generated due to the oxidation of molten substances. However, although only a small amount of CH_4 was generated in this experiment, it was noted that CH_4 could be generated by the reaction of CO or CO_2 with H_2 at lower temperatures in the piping of the reactor coolant system 5).

The oxidation ratio in the QUENCH-07 and QUENCH-09 experiments was 20% and 50%, respectively, and the contribution rate to the total quantity of H_2 generation was 2.4% and 2.2%, respectively. The quantity of H_2 generated was 0.4 kg from QUENCH-09 and 0.12 kg from QUENCH-07; the reason for the difference was due to the steam starvation that was simulated by reducing the steam flow to the test zone from 50 g/s to 3.3–0.4 g/s for 11 min before reflooding in the QUENCH-09 experiment, while this reduction did not occur in the QUENCH-07 experiment 5). A plausible explanation for the increase in hydrogen generation is that, when the oxidized fuel rod is left in a condition where the steam supply is limited, the ZrO_2 layer surrounding the cladding tube decreases and becomes Zr because of the reduction, which allows oxygen to be captured easily when the steam supply resumes 5).

5. FPT-3 Experiment (IRSN) 9, 16-18)

The FPT-3 experiment was conducted within the framework of the international severe accident research program PHEBUS/FP in the Cadarache Research Center at the initiative of IRSN/France and the European Community (EC). The goal was to investigate the melting of fuel, release of radioactive materials from fuel, and transportation of radioactive materials in the reactor coolant system and containment.

In the PHEBUS/FP experiment, 20 fuel rods (1 m long) and one simulated control rod were heated by nuclear fission in the PHEBUS reactor, and the released radioactive materials were captured in a steam generator or containment vessel that simulated a 900 MWe PWR at a 1/5,000 scale. The cross-section and front view of the simulated reactor core are shown in **Figure 7**, and the experiment matrix is shown in **Table 1**.

The FPT-3 experiment aimed at investigating the influence of B_4C pellet control rods used in EPR and was conducted in 2004 as the fifth and final experiment in the same program. The main finding was the observation of a significant increase in the gaseous (organic) iodine content in the simulated containment vessel compared to other PHEBUS/FP experiments that used S-I-C control rods. The organic iodine (CH_3I) content in the gaseous iodine in the simulated containment vessel was approximately 5% when the fuel was damaged, the maximum content was approximately 30%, but was kept within 10–20% for an extended period afterwards

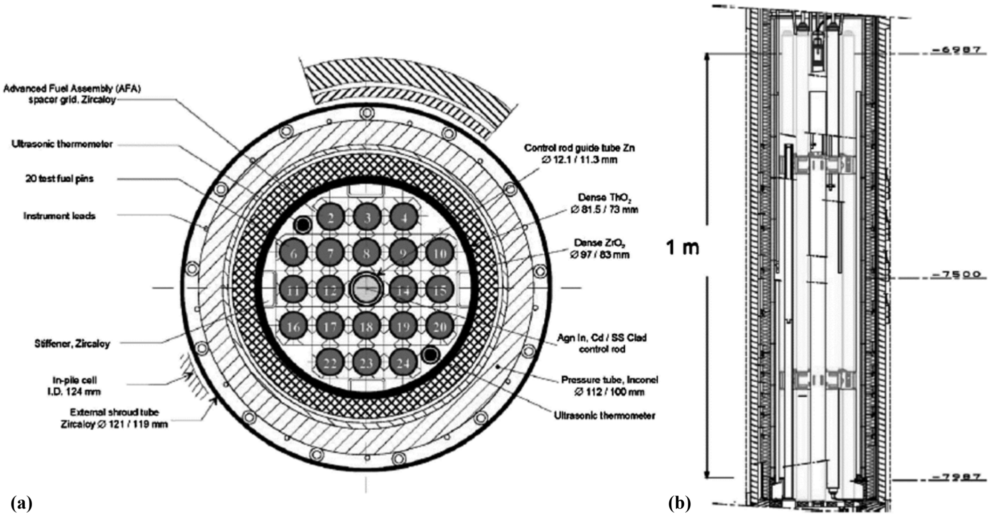

Figure 7 Cross-section and front view of simulated reactor core for PHEBUS/FP experiment [16)]

Table 1 PHEBUS/FP experiment matrix

	Fresh Fuel + Irradiated Fuel + Number of Control Rods	Fuel Burnup (GWd/tU)	Atmosphere	Containment Sump Water Condition	Date of Test
FPT-0	20 + 0 +1S-I-C	0	Steam	pH 5, Not Boiling	12/2, 1993
FPT-1	2 + 18 + 1S-I-C	∼23	Steam	pH 5, Not Boiling	7/26, 1996
FPT-2	2 + 18 + 1S-I-C	∼32	Reductive Atmosphere + Boric Acid	pH 9, Boiling	10/12, 2000
FPT-3	2 + 18 + 1B_4C	∼24	Steam	pH 5, Boiling	11/18, 2004
FPT-4	Debris bed without control rod	∼38	Steam + H_2	—	7/22, 1999

S-I-C: silver indium cadmium

(**Figure 8**). Based on a calculation using the SOPHAEROS [21)] thermodynamic chemical equilibrium computation code, an increase in gaseous iodine was predicted. Furthermore, a clogged flow path was observed in the upstream of the simulated steam generator tube during the FPT-3 experiment, but it is highly probable that this was caused by the generation of cesium boric acid ($CsBO_2$) and deposition in the tube [9)].

6. BECARRE Experiment (IRSN) [19)]

The BECARRE experiment was conducted during the period from 2005 to 2010 within the framework of IRSN's International Source Term Program (ISTP) with the objective of investigating the oxidation of B_4C pellets or B_4C-stainless steel eutectic molten material, the collapse process of B_4C control rods, and the challenges faced during the FPT-3 experiment (generation of CH_4 due to oxidation of B_4C).

The test zone of the BECARRE experimental device is shown in **Figure 9**. In this experiment, the 0.6 m long an array of B_4C pellets in a stainless steel cladding tube and zircalloy control rod guide tube were heated up to 1,953 K.

The main findings were the increase in CO and CO_2 generation as a result of the oxidation

Table 2 Comparison of measurements and SOPHAEROS analyses on the percentage of gaseous iodine (to the quantity released from fuel) in simulated containment vessel in PHEBUS/FP experiment [18)]

	Basic analysis	Experiment
Total volatile iodine（% i.b.i.）[a)]		
FPT-0	~2.6	≤2
FPT-1	~0.052	<1
FPT-2-case A[b)]	~0.03	<0.1
FPT-2-case B[b)]	~9	
FPT-3	~18	~27

[a)] Released from the bundle, which reaches the containment vessel in gaseous (as HI) and vapor form (as SnI_2, SnI_4, I_2MoO_2 or others).

[b)] Cases A and B correspond respectively to assumed non-limited and limited Cd release kinetics.

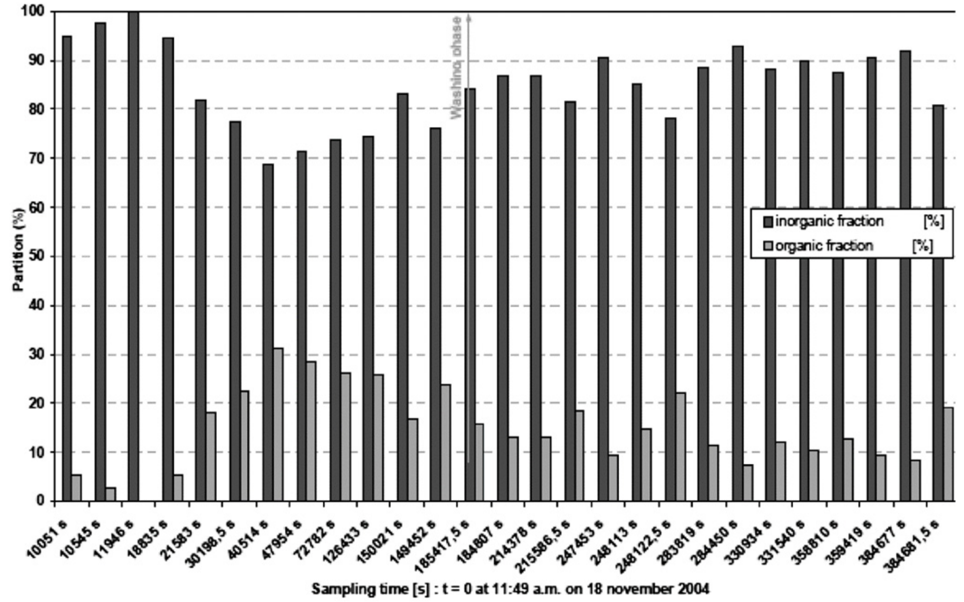

Figure 8 Time-dependent changes in percentage of inorganic iodine and organic iodine observed in simulated containment vessel of FPT-3 experiment [17)]

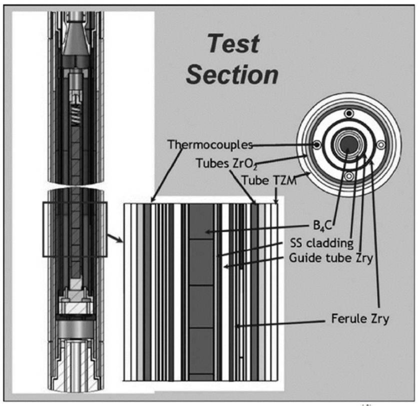

Figure 9 Test zone of BECARRE experimental device [19)]

of B_4C and the decrease in H_2 generation due to the consumption of oxygen by B_4C. However, almost no CH_4 was observed. A study based on the thermochemical equilibrium theory for this outcome found that CH_4 generation hardly occurs under the low pressure conditions (2 bar) that existed during the BECARRE experiment, but occurs readily at temperatures and pressures exceeding 1,500 K and 100 bar, respectively [19)], which supported the very low CH_4 generation observed in the experiment.

Concerning the oxidation of B_4C, the low viscosity molten materials formed by the eutectic reaction between B_4C and the stainless steel cladding flowed down between the inner surface of the stainless steel (SS) cladding tube and outer surface of the B_4C pellets, and solidified at the lower part of the cladding tube where the temperature was 1,073–1,173 K. As a result, not much unoxidized B_4C located above the solidification point was oxidized. In addition, the Zr control rod guide tube that surrounds the SS cladding obstructed contact between unoxidized B_4C and steam. Consequently, hydrogen generation by B_4C oxidation was limited [19)]. A photo of the radial cross-section after the heating experiment on the test zone of the BECARRE experimental device is shown in **Figure 10**.

7. Other Individual Effects Tests

FZK Germany conducted QUENCH-07 and QUENCH-09 experiments, and the Boron Carbide Oxidation (BOX) experiment during the period from 1998 to 2002 to investigate the oxidation behavior of B_4C under high temperatures in the COLOSS (core loss during a severe accident) program [22)], conducted in support of the FPT-3 experiments at the initiative of IRSN as an EC project [8, 23)].

In the experiment, the B_4C specimens (pellets fabricated by FRAMATOME/France, CODEX/Hungary, ESK/Germany, and powder by ESK/Germany) were heated in an inert atmosphere, and the generated gases (H_2, CO, CO_2, and CH_4) were measured by supplying a steam flow after the target temperature was reached. The quantity of generation was in the order of $H_2 > CO_2 > CO > CH_4$. More gas was generated from the powder than from the pellets. H_2 generation increased in proportion to the temperature in the range of 800–1,400°C, and conversely, CH_4 generation reached maximum at 800°C. According to the thermodynamic equilibrium

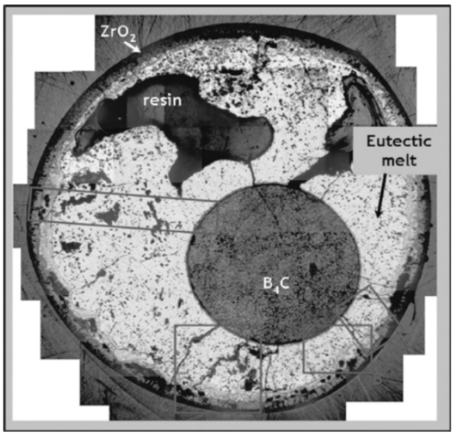

Figure 10 Photo of radial cross-section after heating experiment at 31.1 cm in height from bottom of BECARRE experiment testing zone (areas surrounded by square frame are locations of EPMA analysis) [19)]

calculation, CH_4 generation accelerates at temperatures below 700°C, while CO and CO_2 generation are predominant at temperatures above this value. The transition temperature from CH_4 generation predominant to CO + CO_2 generation predominant was dependent on the oxygen potential, and it shifted toward the high temperature side as the H_2 concentration increased. Furthermore, the generation of gaseous HBO_2 and B_2O_3 increased at temperatures over 1,200°C.

Nagase et al. of the former Japan Atomic Energy Research Institute (JAERI) conducted experimental research on the eutectic reaction between B_4C in the form of powder or pellets and stainless steel (SUS304) in the temperature range of 1,073–1,623 K 24). They discovered that the reaction speed of B_4C (MP 2,620 K) and SUS304 (MP 1,673–1,723 K) approximately followed the Arrhenius type of reaction. The reaction speed between 1,473 K and 1,498 K was noncontiguous due to the formation of a liquid layer on the contacting surface of B_4C and SUS304, and liquification was significantly accelerated near the contacting surface above 1,498 K. In addition, the reaction speed of powder B_4C was higher than that of pellet B_4C.

Furthermore, Minato conducted a thermodynamic chemical equilibrium calculation on the chemical form of iodine and Cs in the reactor cooling system under severe accident conditions and predicted $CsBO_2$ generation 25). In the Wide Range Piping Integrity Demonstration (WIND) study, Shibazaki et al. confirmed by experiment that CsI changes to $CsBO_2$, which has a slightly lower vapor pressure than CsI in the presence of boric acid, and the amount of deposition in the pipe increased compared to the experiment conducted in the absence of boric acid 26).

IV. Experimental Research on Influence of S-I-C Control Materials

In the case of S-I-C absorbers, there is a high possibility that, in the event of a severe accident, the Cd (MT 594 K, BT 1,040 K) gasifies and In (MT 430 K, BT 2,346 K) liquifies before fracture of the cladding tube of the control rod, and when the cladding tube of the control rods fractures (1,550–1,620 K), these elements will blow out as a liquid aerosol 2). Ag (MT 1,235 K, BT 2,483 K) is considered to be released a little later due to a slightly higher melting point 2). **Figure 11** shows a picture of the blown out S-I-C that solidified in the bottom zone of the simulated fuel bundle after a fracture of the cladding tube of the S-I-C control rod (observed in QUENCH-13 experiment). It should be noted that the particles of Ag, In, and Cd that were released in the reactor as aerosols captured the radioactive material and increased deposition on the reactor cooling system piping.

Regarding the relationship with iodine, it was explained that Cd changed to CdI_2 and

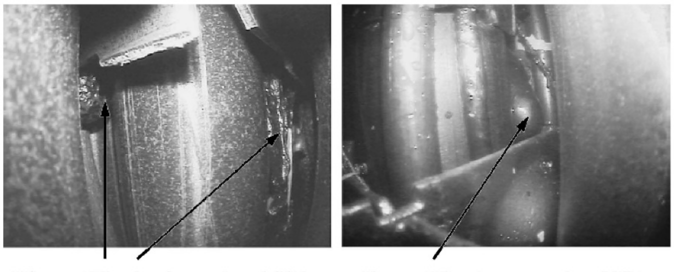

550 mm, AIC melt at lower edge of SG 3 -50 mm, AIC melt at upper edge of SG1

Figure 11 View of blown out Ag, In, and Cd by fracture of cladding tube for S-I-C control rod solidified in the bottom of simulated fuel bundle (observed in QUENCH-13 experiment) 2) condensed in the heat transfer tube of the steam generator. In addition, Ag formed insoluble AgI and inhibited the revolatilization of iodine from the containment sump water.

Additionally, Mo that was generated through nuclear fission formed Cs_2MoO_4 first, and then increased the amount of Cs deposition in the pipe. Furthermore, the possibility of generating CsOH, which was previously considered to be a typical chemical form of Cs, was indicated by the reaction of Cs_2MoO_4 with water 27). On the other hand, in the case of the B_4C control rod, it was noted that not much Cs_2MoO_4 was generated due to consumption by the generation of $CsBO_2$ 18).

A comparison of the influences of S-I-C and B_4C absorbers on the reactor melting process investigated in sections III and IV are listed in **Table 3**.

V. Discussion

1. Weight Ratio of B_4C and Stainless Steel

According to the DF-4 experiment, most of the B_4C relocated to the lower part of reactor core without being oxidized, and no reaction with iodine was observed before the relocation. This is considered to be due to the relocation of B_4C from a high temperature zone to a low temperature zone by being captured by the molten stainless steel after the complete melting of B_4C due to a eutectic reaction with stainless steel. In the reactor core of a BWR, the ratio of stainless steel to B_4C is high. Therefore, it is highly probable that the generation of a large amount of organic iodine that was observed in the FPT-3 experiment, in which the B_4C control rod was simulated, did not take place.

The weight ratio of B_4C to stainless steel could be an important factor in the process of collapse of pellet-type B_4C or powder-type B_4C control rod blades. The ratio of stainless steel (density 7.8 g/cm^3) to B_4C (density 2.5 g/cm^3) is approximately 3.5 (volumes of the two are almost equal) in the FPT-3 experiment and EPR, while that of BWR5/GE is approximately 10. Where the percentage of stainless steel is high, based on the experience in the DF-4 experiment, most of the B_4C will melt into the stainless steel (due to the eutectic reaction) and will be relocated to the low temperature zone in the lower part of the reactor keeping these conditions. Where the

Table 3 Comparison of influence of S-I-C and B_4C absorbers on reactor melting process

	PWR (S-I-C Control Rod)	BWR (B_4C Control Rod)
Failure Temperature of Control Rod	1,550–1,620 K	1,520 K
Behavior of absorbers immediately after failure	Cd (MT 594 K, BT 1,040 K) gasifies and In (MT 430 K, BT 2,346 K) liquifies inside before failure of the cladding tube of control rod and blows out as an aerosol when the cladded tube of the control rods failures. Ag (MT 1,235 K, BT 2,483 K) is released a little later.	The control rods, consisting of B_4C (MT 2,620 K) and stainless steel (MT 1,673–1,723 K), liquify at a temperature lower than the melting points due to the eutectic reaction and start to collapse. The weight ratio of B_4C to stainless steel varies depending on whether B_4C is in powder or pellet form, and B_4C oxidation is influenced by steam.
Influence on source terms	Ag, In, and Cd are released into the reactor in the form of aerosols, the particles grow by capturing FP and accelerate the deposition in the cooling system piping. In relation to iodine, Cd changes its chemical form to CdI_2 and condenses in the steam generator tubes. Ag forms insoluble AgI and inhibits the generation of volatile iodine in the containment vessel.	HBO_2 generated by the oxidation of B_4C combines with Cs and forms $CsBO_2$, which increases the quantity of Cs deposition. Furthermore, CH_4 generated through oxidation of B_4C or the reaction of H_2 with CO or CO_2 reacts with HI or I_2 and forms organic iodine (CH_3I), which increases the source terms (one of the causes is the absence of Ag that inhibits the volatilization of iodine).
Main chemical forms	AgI, CdI_2, Cs_2MoO_4, CsI	$CsBO_2$, CH_3I, CsI, HI 18)

ratio is low, as in the FPT-3 experiment, the integrity of most of the B_4C is maintained in the reactor core, and it is highly probable that the B_4C is oxidized by steam. Furthermore, during the oxidation process, release of iodine and Cs occurs almost at the same time, and it is necessary to consider the influence of these releases. In the BECARRE experiment, the reason why the B_4C pellets were not oxidized to any great extent was because, in addition to the highest temperature of 1,953 K, which was lower than that of the FPT-3 experiment, the absence of fuel rods in the periphery also differed from the configuration of the FPT-3 experiment[19).

Thus, the findings of the experiments using powder- and pellet-type B_4C are different. Therefore, great care must be taken when making predictions using different results. Furthermore, in the FPT-2 experiments with mixed boron in steam, the generation of gaseous iodine was not observed. This requires detailed study in the future.

2. Generation Ratio of Organic Iodine

Not all of the results of the PHEBUS/FPT-3 experiment have yet been disclosed (as of Oct. 2014). An estimation was conducted on the percentage of gaseous inorganic iodine and organic iodine in the containment vessel under severe accident conditions by using the release of almost 100% of the iodine from fuel, as in the FPT-0 experiment, and the information contained in Table 2. Where the fractional release rate of iodine from the fuel in the FPT-3 experiment is assumed to be 100%, the percentage of gaseous iodine in the containment vessel is 27% of the reactor core inventory according to Table 2, and the percentage of organic iodine in the containment vessel is approximately 30%, as shown in Figure 8. Consequently, a maximum of about 8% (i.e., 27% × 0.3) of organic iodine and about 19% of inorganic iodine was present in the containment vessel at the time in the FPT-3 experiment.

Table 4 shows a comparison of the "Guidelines for Safety Evaluation (hypothetical accident, loss-of-coolant accident condition)"[28) in Japan with the evaluation results of the FPT-3 experiment. This table indicates that the percentage of organic iodine in the current "Guidelines for Safety Evaluation" is slightly lower than that obtained in the FPT-3 experiment. However, it is considered too early to adopt this comparison as a basis for making any decision, especially in consideration of the arguments posed in section V-1 as well.

Recently, in the site evaluation guideline subcommittee of the former Nuclear Safety Commission, there was an argument about changing the percentage of organic iodine in the iodine released in the containment from 10% to 1%, with reference to the insights from E.C. Beahm, et. al., bibliography item 10 that the percentage of organic iodine in gaseous iodine is generally less than 1% and that of the new source terms from NUREG-1465 of USNRC[29) (Organic

Table 4 Comparison of "Guidelines for Safety Evaluation (hypothetical accident, loss-of-coolant accident condition)" and the FPT-3 experiment[28)

Guidelines for Safety Evaluation (hypothetical accident, loss-of-coolant accident condition)	FPT-3 Experiment
Percentage of iodine released in the containment vessel: 50%	Percentage of release from fuel 100 % [a)
Inorganic iodine: 50% (fractional release rate) × 0.9 = 45%	Not disclosed
45 % × 0.5 (deposition rate in containment vessel) = 22.5%	Deposition rate in containment vessel: Not disclosed
Gaseous inorganic iodine	
22.5% ÷ 100 (gas-liquid partition coefficient) = 0.225%	Approx. 19%
Organic iodine: 50% (fractional release rate) × 0.1 = 5%	Approx. 8%
Total gaseous iodine: 0.225% +5% = 5.23%	Approx. 27%

[a) The data from the FPT-0 experiment was adopted as a reference because the iodine release rate from the fuel in the FPT-3 experiment had not been disclosed as of Oct. 2014.

iodine is 3% of inorganic iodine) [30]. However, while this change may be appropriate for PWRs, further detailed studies are necessary for application to BWRs.

VI. Summary

B_4C used as absorber of control rods for reactors including BWR, EPR, and VVER, causes a phenomenon during a severe accident that is not observed in PWR, in which silver-indium-cadmium (S-I-C) absorbers are widely used, and may influence the reactor core melting process, H_2 generation quantity, source terms, and other processes. The following insights have been acquired from previous experimental studies:

- During the reactor core melting process, B_4C causes a eutectic reaction with stainless steel-cladding tubes, which liquefies the stainless steel at temperatures less than the melting point of stainless steel and accelerates melting of the reactor core.
- When B_4C is oxidized, similar to the oxidation reaction of Zr, reaction heat and H_2 are generated. Furthermore, most of the separated C changes to CO or CO_2, and some to CH_4. The observed CH_4 generation in the examination of individual effects was minimal, but an unignorable quantity of organic iodine (CH_3I) was observed by the combination of CH_4 and iodine (HI or I_2) in the FPT-3 experiment, which was an integrated experiment. Currently, the processes that generate CH_4 and CH_3I when the oxidation of B_4C and release of iodine occur simultaneously are not sufficiently understood.
- The metaboric acid (HBO_2) produced during the oxidation of B_4C generates cesium boric acid ($CsBO_2$), which increases the deposition of Cs in the reactor coolant system.

Thus, insights have been obtained for several individual phenomena, but the real system-level behavior is not sufficiently understood. The most pressing subject we need to investigate is how the differences in shape and surface area between powder B_4C control rod blades and pellet B_4C control rods, and the difference in weight ratio of B_4C and stainless steel, affect the actual progress of melting, B_4C oxidation, chemical formation of radioactive materials, and release into the environment. It is also expected that further research in this field will provide useful knowledge and insights for reducing uncertainty in understanding how melting of the reactor core progresses and the source terms in the accident at Fukushima, and for establishing the ratio of organic iodine in the safety evaluation.

The author is grateful to Dr. Dana Auburn Powers of Sandia National Laboratories (SNL) US and Dr. Bernard Clément of the Institut de radioprotection et de sûreté nucléaire (IRSN) France who kindly gave him valuable suggestions and comments regarding the differences in the melting behavior of powder B_4C control rod blades and pellet B_4C control rods.

References

1) Nuclear Safety Commission, “US Nuclear Power Station Accident Special Committee - 3rd Report,” May 1981.
2) R. Dubourg, H. Austregesilo, C. Bals et al., “Understanding the behavior of absorber elements in silver-indium-cadmium control rods during PWR severe accident sequences,” *Prog. Nucl. Energy*, 52, 97-198 (2010).
3) D. Magallon, A. Mailliat, J.-M. Seiler et al., ‘‘European expert network for the reduction of uncertainties in severe accident safety issues (EURSAFE),” *Nucl. Eng*. Des., 235, 309-346 (2005).
4) Nuclear Emergency Response Headquarters, “Report of Japanese Government to the IAEA Ministerial Conference on Nuclear Safety–The Accident at TEPCO’s Fukushima Nuclear Power Stations,” June

2011.

5) L. Sepold, G. Schanz, M. Steinbrück et al., “Results of the QUENCH-09 experiment compared to QUENCH-07 with incorporation of B_4C absorber,” *Nucl. Technol*., 154, 107-116 (2006).

6) G. Repetto, O. de Luze, N. Seiler et al., “B_4C oxidation modelling in severe accident codes: Applications to PHEBUS and QUENCH experiments,” *Prog. Nucl. Energy*, 52, 37-45 (2010).

7) L. Barin, *Thermochemical Data of Pure Substances*, VCH Verlagsgesellschaft, Weihelm, Germany (1989).

8) M. Steinbrück, A. Meier, U. Stegmaier et al., “Oxidation of B4C at high temperatures,” *11th Int. Conf. on Nucl. Eng. (ICONE11)-36063*, Tokyo (2003).

9) T. Haste, F. Payot, C. Dominguez et al., “Study of boron behavior in the primary circuit of water reactors under severe accident conditions: A comparison of Phebus FPT3 results with other recent integral and separate-effects data,” *Nucl. Eng. Des*., 246, 147-156 (2012).

10) E. C. Beahm, C. F. Weber, T. S. Kress et al., *Iodine Chemical Forms in LWR Severe Accidents*, NUREG/CR-5732 (1992).

11) R. O. Gauntt, R. D. Gasser, L. J. Ott, *The DF-4 Fuel Damage Experiment in ACRR with a BWR Control Blade and Channel Box*, NUREG/CR-4671 (1989).

12) R. O. Gauntt, R. D. Gasser, “Results of the DF-4 BWR control blade-channel box test,” *Proc. Eighteenth Water Reactor Safety Information Meeting*, NUREG/CP-0114, 2, 25-40 (1990).

13) R. O. Gauntt, L. L. Humphries, *Final Results of the XR2-1 BWR Metallic Melt Relocation Experiment*, NUREG/CR-6527 (1997).

14) P. Hofmann, M. Markiewicz, J. Spino, “Reaction behavior of B_4C absorber material with stainless steel and zircaloy in severe LWR accidents,” *Nucl. Technol*., 90, 226-244 (1990).

15) A. Miassoedov, C. Homann, G. Schanz et al., “Results of the QUENCH-09 experiment on the investigation of the cool down behavior of the fuel rod simulators,” *11th Int. Conf. on Nucl. Eng*. (ICONE11)-36035, Tokyo (2003).

16) B. Clément, N. Girault, G. Repetto et al., “LWR severe accident simulation: synthesis of the results and interpretation of the first Phebus FP experiment FPT0,” *Nucl. Eng. Des*., 226, 5-82 (2003).

17) F. Payot, P. March, B. Biard et al., *Phebus FPT3: Main Relevant Results Likely to Impact Safety*, EUROSAFE, http://www.eurosafe-forum.org/files/seminar1_01_2007.pdf.

18) N. Girault, C. Fiche, A. Bujan et al., “Towards a better understanding of iodine chemistry in RCS of nuclear reactors,” *Nucl. Eng. Des*., 239, 1162-1170 (2009).

19) O. de Luze, “Degradation and oxidation of B_4C control rod segments at high temperatures. A review and code interpretation of the BECARRE program,” *Nucl. Eng. Des*., 259, 150-165 (2013).

20) R. C. Schmidt, *MERIS: A Model for Melt Relocation in Core Structures of Nuclear Reactors during Severe Accident Conditions*, NRC FIN L-2452, Sandia National Laboratories, Albuqerque, NM, Oct. 1993.

21) A. Bujan, L. Ammirabile, J. Slaby, “ASTEC V2.0 computational evaluation of source term and its chemical forms under accidental conditions during mid-loop operation,” *Prog. Nucl. Energy*, 53, 438-448 (2011).

22) B. Adroguer, F. Bertrand, P. Chatelard et al., “Core loss during a severe accident (COLOSS),” *Nucl. Eng. Des*., 235, 173-198 (2005).

23) M. Steinbrück, A. Meier, U. Stegmaier et al., *Experiments on the Oxidation of Boron Carbide at High Temperatures*, FZKA 6979 (2004).

24) F. Nagase, H. Uetsuka, T. Otomo, “Chemical interactions between B_4C and stainless steel at high temperatures,” *J. Nucl. Mater*., 245, 52-59 (1997).

25) K. Minato, “Thermodynamic analysis of cesium and iodine behavior in severe light water reactor accidents,” *J. Nucl. Mater*., 185, 154-158 (1991).

26) H. Shibazaki, Y. Maruyama, T. Kudo et al., “Revaporization of a CsI aerosol in a horizontal straight pipe in a severe accident condition,” *Nucl. Technol*., 134, 62-70 (2001).

27) M. P. Kissane, I. Drosik, “Interpretation of fission-product transport behaviour in the Phebus FPT0 and FPT1 tests,” *Nucl. Eng. Des*., 236, 1210-1223 (2006).

28) Nuclear Safety Commission, “Regulatory Guide for Reviewing Safety Assessment of Light Water Nuclear Power Reactor Facilities,” Published in Aug.30. 1990, Latest revision Mar. 29. 2001.

29) U. S. Nuclear Regulatory Commission, “Accident Source Terms for Light-Water Nuclear Power Plants,” NUREG-1465 (1995).

30) Special Committee of Nuclear Safety Standards/Guidelines, Subcommittee to discuss “Regulatory Guide for Reviewing Nuclear Reactor Site Evaluation and Application Criteria,” and the revisions on relevant safety examination guidelines “Interim Report of Investigation and Examination Statuses,” Mar. 30. 2010.